

The sulphur depletion problem in molecular clouds: The H₂S case

David Navarro-Almaida¹

¹Observatorio Astronómico Nacional, IGN-CNIG, Calle Alfonso XII, 3-5, 28014 Madrid, Spain

Abstract.

Sulphur is one of the most abundant elements in the Universe and plays a crucial role in biological systems. However, sulphuretted molecules in the ISM are not as abundant as expected and there is no clear answer of where the missing Sulphur is yet. To shed light onto this open question, we focus our attention on the chemistry of H₂S, thought to be an important reservoir of Sulphur and formed mainly by grain-phase reactions. To understand the formation of H₂S, the growth of ices, and the chemical desorption process, we study the CO, CH₃OH, N₂H⁺, and H₂S abundances towards Barnard 1b, a Sulphur-rich cloud hosting a first Larson core. We look for correlations between gas-phase abundances of H₂S and CH₃OH that better constrain the location of the CO snowline in dark cores. Finally, this provides additional data to benchmark models for a deeper insight on the chemical desorption process and its efficiency.

1 Introduction

Despite being one of the most abundant elements in the Universe, with an elemental solar abundance of S/H $\sim 1.35 \times 10^{-5}$, sulphur-bearing molecules are not as abundant as expected. While in diffuse clouds and PDRs the sulphur abundance is found to be close to the cosmic value [1], sulphur is thought to be depleted inside molecular clouds by a factor of 1000 compared to its estimated cosmic abundance [2]. Due to the high hydrogen mobility in the ice matrix, the sulphur atoms depleted in interstellar ice mantles are expected to form H₂S preferentially. Therefore, H₂S is a candidate for the main sulphur reservoir in dark cores [3]. In [4], we found H₂S to be the main sulphur reservoir in TMC 1 and Barnard 1b, released into the gas phase by chemical desorption. The chemical modeling of this molecule allowed us to conclude that it is a tracer of the snow-line in these regions, as the gas-phase abundance at higher extinctions is reduced due to the lower chemical desorption efficiencies. The observed abundances are reproduced with the models using a cosmic elemental Sulphur abundance and allowing an order of magnitude of uncertainty. This work is a follow-up of [4] where we used a subset of the GEMS database [5] and complementary CO and methanol observations to investigate the H₂S and methanol abundances, the interplay of CO, methanol, and the snow-line, and the mechanisms and efficiencies of formation of methanol and H₂S in Barnard 1b.

2 Observations: Barnard 1b

Barnard 1 is a young, intermediate-mass star forming cloud, embedded in the western sector of the molecular cloud complex Perseus (see Fig. 1). It hosts several dense cores in different

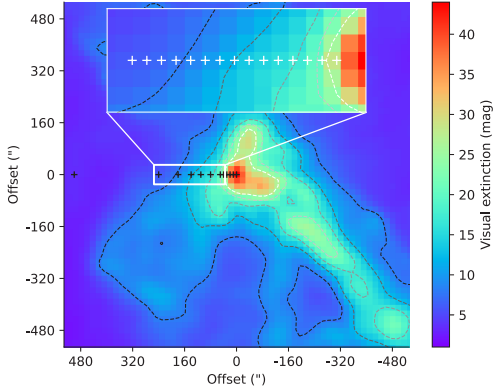


Figure 1: Extinction map of Barnard 1b with the observed positions (white crosses) and GEMS positions (black crosses) [4].

Table 1: Observed lines

Molecule	Line	Freq. (GHz)
^{13}CO	$1 \rightarrow 0$	110.201
C^{18}O	$1 \rightarrow 0$	109.782
H_2S	$1_{1,0} \rightarrow 1_{0,1}$	168.763
N_2H^+	$1 \rightarrow 0$	93.174
CH_3OH	$\text{E}2\ 2_{1,2} \rightarrow 1_{1,1}$	96.739
CH_3OH	$\text{E}1\ 2_{0,2} \rightarrow 1_{0,1}$	96.745
CH_3OH	$\text{A}^+\ 2_{0,2} \rightarrow 1_{0,1}$	96.741
CH_3OH	$\text{A}^+\ 1_{0,1} \rightarrow 0_{0,0}$	48.372

evolutionary stages, out of which Barnard 1b is the youngest. Barnard 1b has a rich chemistry characterized by large abundances of sulphur-bearing compounds. This work uses a subset of the GEMS database and complementary IRAM 30m observations of the lines shown in Table 1. Additionally, $\text{CH}_3\text{OH A}^+ 1_{0,1} \rightarrow 0_{0,0}$ data from the Yebes 40m telescope was observed at the lowest extinctions.

3 Analysis and results

For a better understanding of the depletion of species, the presence of the snow-line, and the formation of H_2S and CH_3OH , we derived the column densities of the species listed in Table 1, and the physical properties at every position. First, we obtained the hydrogen nuclei number density and the methanol column density using the methanol lines shown in Table 1. To do so, we used the radiative transfer code RADEX with the most up-to-date collisional coefficients for e-methanol and a-methanol [6]. Assuming the gas temperature profile obtained in [4], the intensity ratio $W(\text{E}2\ 2_{1,2} \rightarrow 1_{1,1})/W(\text{E}1\ 2_{0,2} \rightarrow 1_{0,1})$ provides an estimation of the hydrogen nuclei number density that is then used to compute the column density of both methanol species. In positions where at least one of these lines were not detected, we performed additional observations with the Yebes 40m telescope to obtain the density from the $W(\text{A}^+\ 1_{0,1} \rightarrow 0_{0,0})/W(\text{A}^+\ 2_{0,2} \rightarrow 1_{0,1})$ intensity ratio. The column density of the rest of the species are derived fitting the integrated intensity of the lines.

The resulting abundances are shown in Fig. 2. We first notice the presence of H_2S in the gas phase at the most external positions where CH_3OH is not detected. This is compatible with an early depletion of Sulphur atoms onto grain surfaces [7], before significant depletion of CO. Since reactions with CO are the main destruction path of N_2H^+ [8], when CO depletion occurs, N_2H^+ starts increasing its abundance. At the same time, CH_3OH also starts increasing, slightly, its abundance, as it is mainly formed by hydrogenation of depleted CO. The depletion of CO is linked to ice growth which, in turn, reduces the desorption efficiency of molecules formed via grain-phase reactions. This is the case of H_2S , whose abundance decreases as ^{13}CO starts depleting and methanol and N_2H^+ increase their abundances.

Methanol, like H_2S , is also produced more efficiently through grain-phase reactions in cold core conditions. However, the gas abundance of methanol does not seem to be affected

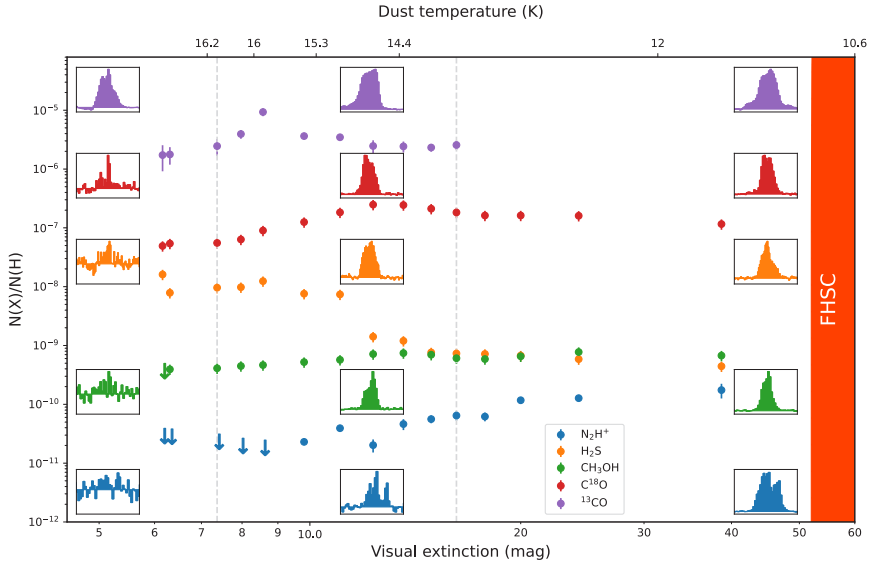


Figure 2: Abundances $N(X)/N(H)$ of ^{13}CO , C^{18}O , H_2S , CH_3OH , and N_2H^+ molecules as a function of the visual extinction and dust temperature.

by the decreasing desorption efficiency expected by grain growth. The desorption of COMs like methanol in grains covered by CO ice has been discussed in several works [9]. Current chemical models do not consider a detailed chemical composition of the outermost layers of ices. It is likely that these layers, containing mainly depleted CO, could enhance the chemical desorption of COMs [9] while also reducing the desorption efficiencies of other molecules like H_2S . Surface-dependent parameters like the diffusion rate of hydrogen through the ice matrix have also been found to have a great impact in the methanol production [10].

Now we explore the role of ices in the production of H_2S and methanol. The chemical code NAUTILUS [11], using the densities obtained here and the parameters described in [4], yields the abundances shown in Fig. 3. This model adjusts the desorption efficiency with the ice growth, being at its highest when no ice is present. The efficiency of desorption is reduced as ice grows at higher extinctions. The desorption schemes used in the model are described in [4]. The model results for H_2S (Fig. 3) are in good agreement with the observations, with high desorption efficiencies and low desorption efficiencies best describing low and high extinction areas, respectively, as a consequence of the build-up of ices towards the interior of the core. The model does not however reproduce the observations of methanol, even in a scenario of early chemistry at 10^5 yr (Fig. 3), since it underestimates its gas-phase abundance. In the following section we discuss several ideas that may be behind this disagreement.

4 Discussion and summary

The chemistry of sulphur and COMs are tightly related to grain-phase reactions. The chemical desorption process is crucial for the incorporation of these species into the gas-phase. Even though H_2S and methanol are mainly formed via chemical desorption, we have revealed great differences between the distribution of their gas-phase abundances.

- Gas-phase abundance of H_2S is anti-correlated with the ice growth expected when CO is being depleted. Our model, which takes into account different desorption schemes as

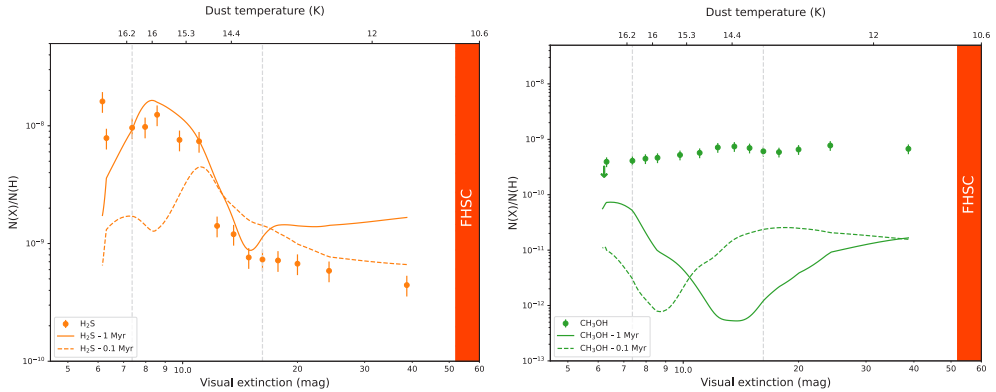


Figure 3: *Left:* Observed H_2S abundances (orange dots) and model predictions at two different times: 1 Myr (solid) and 0.1 Myr (dashed). *Right:* Observed methanol abundances (dark green dots) and model predictions at two different times: 1 Myr (solid) and 0.1 Myr (dashed).

ice grows, shows a good agreement with the observations, thus suggesting that the H_2S gas-phase abundance traces the CO snowline. Other possibility that may help explain the observed abundance profile is that H_2S , in presence of depleted CO, reacts with it forming other compounds such as OCS and therefore no H_2S is released to the gas phase [12].

- Methanol gas-phase abundance is correlated with CO depletion, in agreement with the formation of methanol by hydrogenation of depleted CO. The measured abundances of methanol and H_2S follow different behaviors despite having similar formation pathways. As discussed previously, CO-ices could enhance the desorption of COMs, although this is yet to be confirmed. Recent results also suggest alternative routes of methanol formation that need to be incorporated into chemical networks [13].
- Finally, uncertainties in the physical structure, grain sizes, and the dynamical behavior may explain the striking differences in methanol and H_2S gas-phase abundances.

References

- [1] D.A. Neufeld, B. Godard, M. Gerin, et al, *A&A* **577**, A49 (2015), 1502. [05710](#)
- [2] M. Agúndez, V. Wakelam, *Chemical Reviews* **113**, 8710 (2013), 1310. [3651](#)
- [3] T.H.G. Vidal, J.C. Loison, A.Y. Jaziri, et al, *MNRAS* **469**, 435 (2017), 1704. [01404](#)
- [4] D. Navarro-Almaida, R. Le Gal, A. Fuente, et al, *A&A* **637**, A39 (2020), 2004. [03475](#)
- [5] A. Fuente, D.G. Navarro, P. Caselli, et al, *A&A* **624**, A105 (2019), 1809. [04978](#)
- [6] D. Rabli, D.R. Flower, *MNRAS* **406**, 95 (2010)
- [7] S. Cazaux, H. Carrascosa, G.M. Muñoz Caro, et al, *A&A* **657**, A100 (2022), 2110. [04230](#)
- [8] P. Caselli, C.M. Walmsley, M. Tafalla, et al, *ApJ* **523**, L165 (1999)
- [9] A.I. Vasyunin, P. Caselli, F. Dulieu, et al, *ApJ* **842**, 33 (2017), 1705. [04747](#)
- [10] A. Punanova, A. Vasyunin, P. Caselli, et al, *ApJ* **927**, 213 (2022), 2112. [04538](#)
- [11] M. Ruaud, V. Wakelam, F. Hersant, *MNRAS* **459**, 3756 (2016)
- [12] M. el Akel, L.E. Kristensen, R. Le Gal, et al., *A&A* **659**, A100 (2022)
- [13] J.C. Santos, K.J. Chuang, T. Lamberts, et al, arXiv e-prints arXiv:2205.12284 (2022), 2205. [12284](#)